Chinese Journal of
POLYMER SCIENCE

FEATURE ARTICLE

https://doi.org/10.1007/s10118-018-2087-x
Chinese J. Polym. Sci. 2018, 36, 297–305

Directional Photo-manipulation of Self-assembly Patterned Microstructures

Wei Wang, Fei Gao, Yuan Yao, and Shao-Liang Lin*

Shanghai Key Laboratory of Advanced Polymeric Materials, Key Laboratory for Ultrafine Materials of Ministry of Education, School of Materials Science and Engineering, East China University of Science and Technology, Shanghai 200237, China

Abstract Highly intricate surface architectures derived from patterned polymer microstructures have received increasing concern in recent years. Directional photo-manipulation (DPM) of azopolymers is one of the effective strategies to tune the patterned polymer microstructures through directional mass migration (DMM) upon polarized light illumination. In this feature article, we emphasize the latest advances of DPM on azopatterns created by self-assembly. The mechanism of DMM, the photo-manipulation performance, and functions of manipulated patterns are introduced in sequence. As presented, DPM can manipulate the as-prepared microstructures feasibly by taking the advantages of non-contacting and nondestructive characters. Moreover, the challenges and opportunities of DPM strategy are discussed in conclusion.

Keywords Self-assembly; Directional photo-manipulation; Surface patterning; Azopolymer

Citation: Wang, W.; Gao, F.; Yao, Y.; Lin, S. L. Directional Photo-manipulation of Self-assembly Patterned Microstructures. Chinese J. Polym. Sci. 2018, 36(3), 297–305.

INTRODUCTION

Surface patterning with polymeric materials is promising especially in micro-electronics, information processing and storage, nano/microfluidic devices, and biological detection[1–3]. In general, two strategies known as "top-down" and "bottom-up" are commonly adopted for polymer patterning. In the top-down approach, patterns are written or transferred onto substrates directly, and subsequently engraved by optical lithography, e-beam lithography, soft lithography and nanoimprint lithography, *etc*[4]. Alternatively, "bottom-up" approach employs the polymer components to build ordered patterning architecture mainly through the self-assembly of block copolymers, polymer nanocrystals, clusters, nanocomposites and colloidal particles[5, 6]. By combining self-assembly with some top-down methods, various polymeric patterns with multifarious functions could be obtained through the post modification for reshaping the pristine structure to desired architectures[7–9].

The incorporation of environmental-sensitive components with polymeric patterns enables stimuli transformation for fabricating intricate architectures[10, 11]. As an attractive strategy, azobenzene moieties have been adopted into polymer patterns due to their reversible photo-responsiveness upon ultraviolet (UV) or visible light irradiation in the past decade[12, 13]. For example, the directional photo-manipulation (DPM) of azopolymers has also been extended from self-assembled micelles to patterns by taking the advantage of photo-induced directional mass migration (DMM) of azobenzene moieties[14, 15]. This strategy features the unique directionality and maneuverability to adapt the morphology manipulation of small surface features[16]. Very recently, a series of patterned azopolymer structures were prepared by self-assembly or judiciously combining polymeric self-assembly with "top-down" methods. By exerting polarized light on these azo-patterns, the obtained structures could be deterministically manipulated into desired architectures. In addition, surface properties such as anisotropic arrangement and particular shape were obtained on these patterns, which enabled some unique functions and applications. In this feature article, the mechanism of photo-induced mass migration of azobenzene is introduced in the first part. Subsequently, we devote our efforts to review the recent advances on the DPM of self-assembly created azo-patterns. The functions and applications of these manipulated patterns are introduced in the third section. Lastly, conclusions and outlook of this area are presented.

DIRECTIONAL MASS MIGRATION OF AZOMATERIALS

As a typical photochromic group, azobenzene has drawn great attention for its unique optical properties based on photo-isomerization (see Fig. 1)[17, 18]. Azobenzene exists in two isomer forms. One is thermally stable *trans*, and the other is metastable *cis*. Typically, t*rans* isomer features strong π-π^* absorption band in UV radiation wavelength range, whereas *cis* isomer has slightly weaker n-π^* absorption band in visible

* Corresponding author: E-mail slin@ecust.edu.cn
Invited paper for special issue of "Supramolecular Self-Assembly"
Received September 28, 2017; Accepted November 6, 2017; Published online December 20, 2017

© Chinese Chemical Society
Institute of Chemistry, Chinese Academy of Sciences
Springer-Verlag GmbH Germany, part of Springer Nature 2018

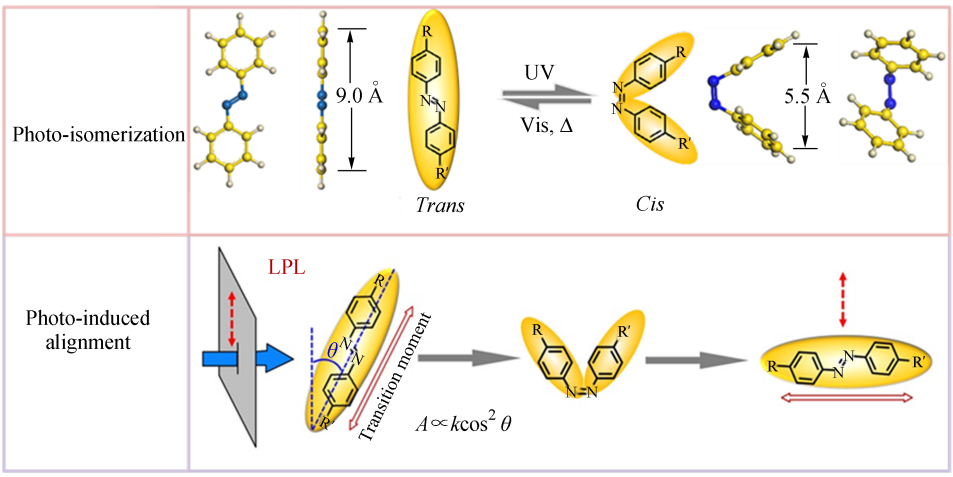


Fig. 1 Scheme of photo-isomerization and photo-induced alignment of azobenzen moieties

light wavelength range[19]. Upon UV light (λ ~ 365 nm) irradiation, *trans* isomer can be readily transformed to *cis* form. This isomerization is reversible when the *cis* isomer is exposure to visible light (~450–500 nm) or to be heated[20]. Photo-isomerization of azobenzene moieties drastically influences the geometry, polarity, and electronic properties of azopolymers[21]. Under the isomerization, rod shaped *trans* isomer which is approximately 9 Å in length turns into a "kinked" shaped *cis* isomer with the length around 5.5 Å, showing an obvious length reduction around 3.5 Å[22]. Another significant distinction between the two isomers is their capability to absorb polarized lights. *Trans* isomer selectively absorbs polarized light, and the absorbance (A) is tightly related to the angle θ between their transition moments and light polarization direction ($A \propto k\cos^2\theta$), as depicted in Fig. 1. In contrast, *cis* isomer does not feature selective absorbance. Upon polarized light irradiation, the *trans* isomer whose transition moments have projection along light polarization direction is activated and transformed to *cis* state, and the *trans* isomer with the transition moments perpendicular to polarization direction is not triggered[23]. Therefore, when exposed to blue-green light, *trans*-to-*cis* and *cis*-to-*trans* isomerization will simultaneously occur in azobenzene molecules due to the overlap in their optical absorption spectra[24]. Combining the polarization-selective *trans*-to-*cis* isomerization with unselective *cis*-to-*trans* reverse isomerization, azobenzene groups gradually reorient to a plane orthogonal to the polarized direction, which is known as photo-induced alignment (also as Weigert effect) in Fig. 1[25].

The isomerization of azobenzene molecules gives rise to additional free volume and dramatically decreases the viscosity of local area, and therefore exerts plasticization effect and increases the chain mobility (known as photo-fluidization effect). Furthermore, the isomerization produces a coherent force on neighbouring molecules to induce cooperation orientation in local area[26]. In consequence, polarized illumination produces a stream of randomly occurring isomerization accompanied with photo-fluidization on azomaterials. Simultaneously, light polarization can induce the photo-alignment of *trans* isomers and cooperative orientation of neighbouring molecules in the local area. The synergy of these effects enables the DMM of the whole azostructure.

Azobenzene moieties in azopolymers can appropriately inherit above excellent photo-responsive properties, including photo-isomerization, photo-induced alignment and photo-induced DMM (also called mass transportation)[27, 28]. Therefore, the DMM phenomenon can be visualized experimentally on patterned film of azopolymer (see Figs. 2a–2d)[29]. Herein, two perpendicular canals were created by scanning probe microscopy on a smooth azofilm. Upon linearly polarized light (LPL) irradiation, the canal 1 which is vertically aligned to polarization direction gradually coalesced. In contrast, the width of parallel canal 2 with respect to polarization direction increased, indicating that the azobenzene moieties tended to migrate along the polarized direction. Another example is the directional reshaping of line arrays. The spacing of azopolymer lines gradually decreased along the polarization direction as a result of DMM (Figs. 2e–2h)[15]. The unprecedented directional property has been implemented to manipulate the microstructure of azobenzene for its controllable, non-contacting and nondestructive characters.

DIRECTIONAL PHOTO-MANIPULATION OF SELF-ASSEMBLY PATTERNED AZOPOLYMER MICROSTRUCTURES

Based on the self-assembly of azopolymer, various microstructures have been readily fabricated and further tuned by DPM through the DMM of azobenzene. By changing the type of light polarization, polarization direction, and irradiation period precisely, the pristine patterns could be successively reshaped to intricate architectures. In addition, unique size dependence was observed in DPM processing because of the superficial absorbance property of azomaterials.

Linearly Polarized Light Based Manipulation

Breath figure is a facile and high-throughput method to prepare ordered polymer films[30, 31]. Recently, DPM technique is in conjunction with breath figure processing to

https://doi.org/10.1007/s10118-018-2087-x

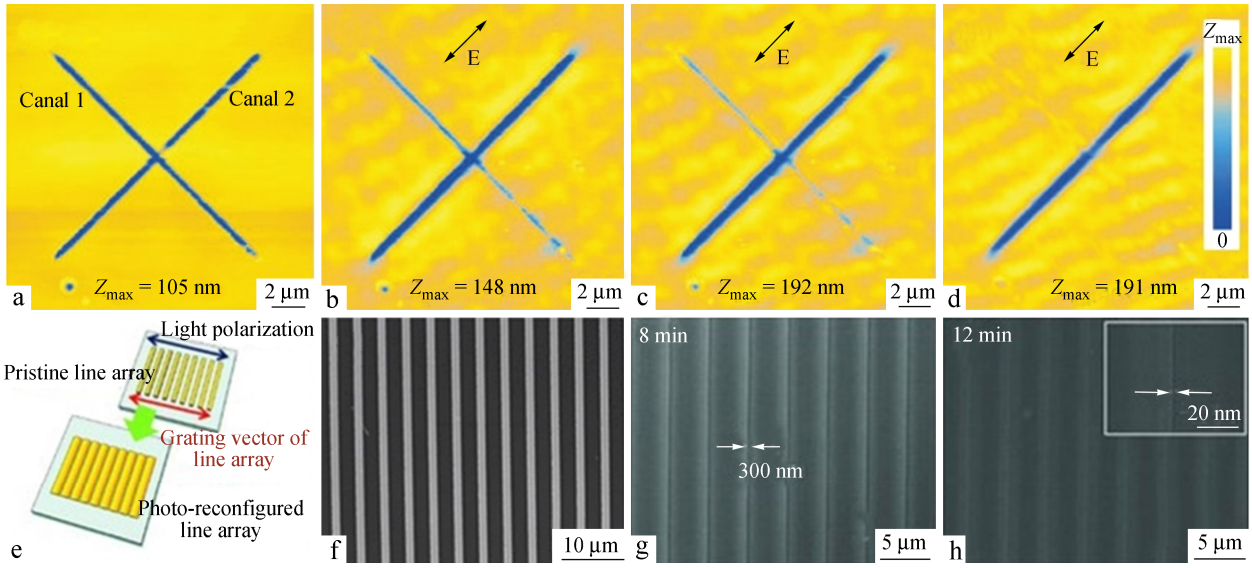


Fig. 2 Directional photo-induced movements of azopolymers visualized by LPL irradiation on films
(a–d) Using a thin film with two perpendicular canals produced with a scanning-force microscope tip: (a) an atomic-force micrograph of pristine film; (b–d) images taken after 30, 150, and 195 min irradiation (532 nm, 60 mW/cm^2), respectively (Reproduced with permission from Ref. [29]; Copyright (2005) Nature Publishing Group); (e–h) Using a patterned film with line-stripe arrays: (e) schematic diagrams of LPL irradiation on the azo-arrays; (f) scanning electron microscopy (SEM) image of pristine line arrays; (g) SEM image after 8 min irradiation; (h) SEM image after 12 min irradiation (Reproduced with permission from Ref. [15]; Copyright (2011) John Wiley and Sons, Inc.)

fabricate microporous films with finely tuned features. In this work, diblock azopolymer poly(4-vinylpyridine)-block-poly[6-[4-(4-butylphenylazo)phenoxy]hexyl methacrylate] (P4VP-*b*-PAzoMA) was selected to prepare porous films through breath figure process (Fig. 3a)[32]. The obtained monolayer breath figure arrays (BFAs) with highly ordered hexagonal arranged pores are shown in Figs. 3(b) and 3(c). Vertical incident LPL at 450 nm was subsequently implemented to manipulate the porous structure. Based on the periodicity and anisotropy of honeycomb structure, two characteristic polarization directions were chosen to perform DPM (Fig. 3d). The one parallel to hexagonal walls was defined as *V* direction, and the other perpendicular to hexagonal walls was named *S* direction. Round pores in BFAs could be converted into rectangular, rhombic structures upon *V* or *S* direction irradiation for 30 min, respectively (Figs. 3e and 3f). In addition, film with parallelogram shaped pores was prepared after irradiation along a direction between the *S* and *V* direction. Further increasing the irradiation time to 2.0 h, the porous structure would collapse vertically.

By this way, a series of BFAs with various morphologies were prepared by simply changing the fabrication condition. Intriguing patterns with holes of elliptical shape or long slit were readily created by subsequent DPM on these BFAs[33]. In addition to vertical incident LPL, oblique incidence LPL was also applied on the DPM of honeycomb patterns. Superficial rectangle or rhombic pores were also obtained under the LPL irradiation along *V* or *S* direction for 30 min. Besides, inner walls in the irradiation plane were aligned to form asymmetrical structures due to the horizontal projection of polarization. In contrast, the walls perpendicular to the irradiation plane were not influenced by the slant direction of irradiation. Accordingly, the inner asymmetrical structures were created by DPM under slantwise LPL irradiation. DPM technique in conjunction with breath figure processing provides a platform for preparing intricate micropatterned films without direct writing, imprint, and expensive lithographic techniques.

In another research, the combination of colloidal self-assembly and soft lithography was applied to prepare azopolymer arrays as depicted in Fig. 4(a)[34]. The pristine hexagonal-close-packed (HCP) pattern was made of polystyrene colloidal spheres through solvent evaporation induced self-assembly. Next, reactive ion etching (RIE) technique was adopted to turn the HCP pattern into non-close packed (NCP) one. After duplicated twice through soft lithography, a large-area ordered azobenzene homopolymer array was obtained (Fig. 4b). The array was apt to transform into different shapes, sizes and alignments by tuning the irradiation time and polarization direction of LPL irradiation. Typically deformed pattern after irradiation for 30 min along *S*′ direction (parallel to the side of cell) is shown in Fig. 4(c), and a large-area uniform pattern with identical spindle-like protrusions is observed. Irradiation time played a crucial role in the shape variation of protrusions on the micropattern. At the beginning stage, both elongation along the polarization direction and shrunk along the orthogonal direction were observed due to a diffusive effect. After illuminated for a longer time, the protrusions preferred to expand rather than elongation because of the slow collapse of the whole protrusion induced by photo-fluidization. Therefore, flat and ellipsoid-like protrusions were obtained. If the irradiation time was long enough (*ca.* 300 min), the protrusions would interconnect along the polarization direction (Fig. 4d). Furthermore, secondary irradiation was introduced to manipulate the arrays to form complex 3D morphologies (Figs. 4e and 4f). By tuning the secondary rotation angle of LPL to 45° or 90°, near-hexagon array or near-rhombus array

https://doi.org/10.1007/s10118-018-2087-x

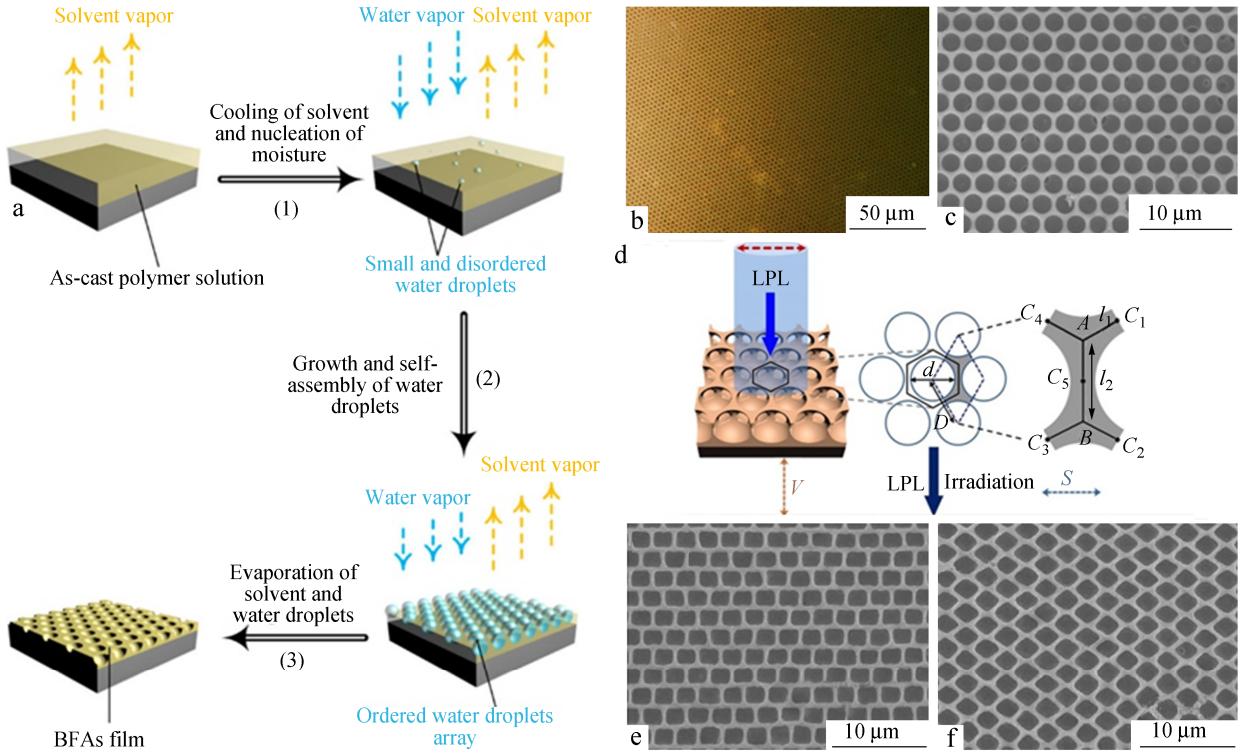


Fig. 3 (a) Scheme of breath figure process (Reproduced with permission from Ref. [31]; Copyright (2015) American Chemical Society); (b) Optical microscope image of the honeycomb film formed by azobenzene copolymers; (c) SEM image of the honeycomb structured film; (d) Scheme of two types of LPL irradiation; SEM images of deformed honeycomb films after 30 min irradiation along (e) *V* direction and (f) *S* direction, respectively (Reproduced with permission from Ref. [32]; Copyright (2014) John Wiley and Sons, Inc. Reproduced with permission from Ref. [33]; Copyright (2017) American Chemical Society)

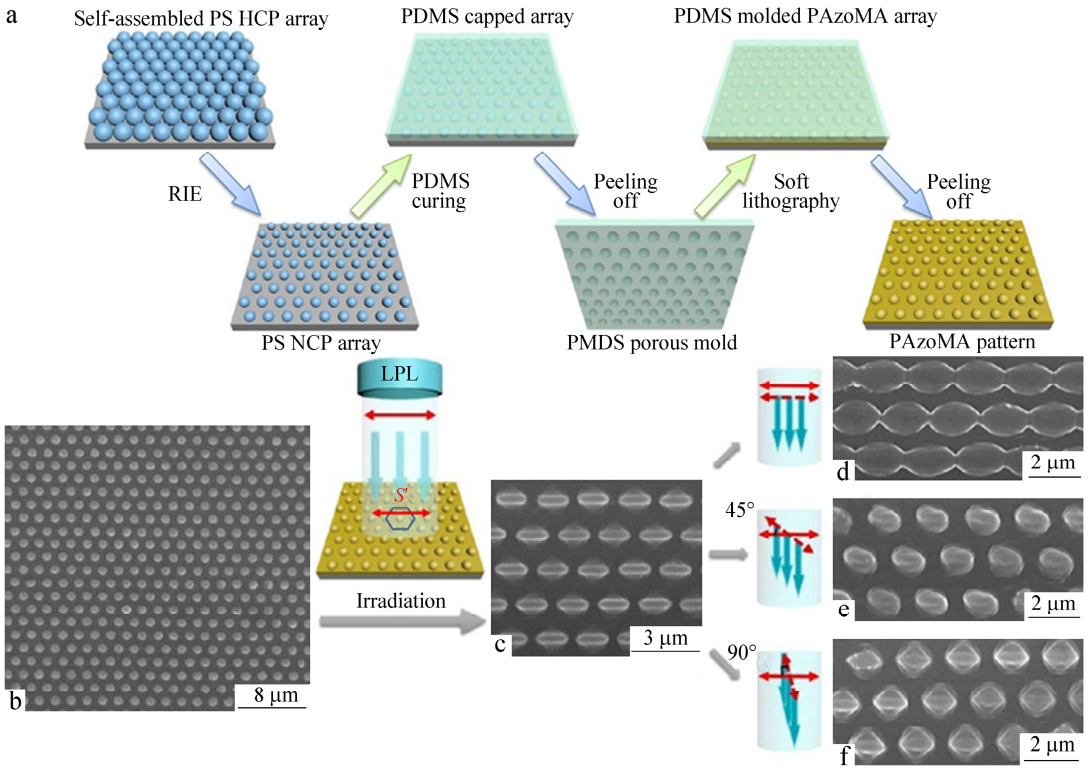


Fig. 4 (a) Schematic illustration of the preparation of PAzoMA hemispherical pattern; SEM images of arrays after processing: (b) the pristine azobenzene homopolymer array and (c) deformed patterns after irradiation along the *S*′ direction for 10 min; (d) deformed patterns after irradiation along the *S*′ direction for 300 min; deformed patterns after secondary LPL manipulation on the pattern in (c) by rotating the polarization angle by (e) 45° and (f) 90°, respectively (Reproduced with permission from Ref. [34]; Copyright (2017) American Chemical Society)

https://doi.org/10.1007/s10118-018-2087-x

could be obtained. Based on these instructive results, artificial design and fabrication of azopolymer patterns with desirable shape, size and alignment were achieved by precisely modulating the irradiation time and polarization orientation.

Circularly Polarized Light-based Manipulation

Different from LPL, circularly polarized light (CPL) does not feature a linear polarized direction because of the clockwise rotating electric field vector[35]. In consequence, CPL gives rise to uniform mass migration toward all radial direction. When CPL was adopted to manipulate the azo-protrusion array, each protrusion migrated homogenously and gradually to cover larger area with irradiation time (Figs. 5a–5c)[34]. This CPL-based manipulation method was also adopted to modify the BFAs[33]. Upon vertical CPL irradiation, obvious increase of wall thickness and decrease of pore size were observed, and the rotational symmetry of porous structures almost preserved during the entire photo-manipulation process. CPL irradiation enlarged the polymeric wall thickness while maintaining the pristine pore shape, which allowed a facile manipulation of wall thickness upon porous films.

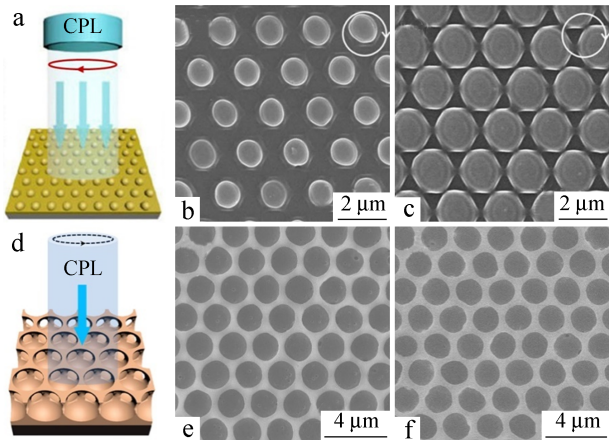


Fig. 5 (a) Scheme of CPL-manipulation on protrusion array; SEM images of reshaped array upon CPL irradiation for (b) 10 min and (c) 720 min, respectively (Reproduced with permission from Ref. [34]; Copyright (2017) American Chemical Society); (d) Scheme of CPL-manipulation on BFAs; SEM images of reshaped array upon CPL irradiation for (e) 30 min and (f) 120 min, respectively (Reproduced with permission from Ref. [33]; Copyright (2017) American Chemical Society)

Size Dependence of Directional Photo-manipulation

In addition to the light-related factors, the size of aggregates also significantly influences on the DPM of azo-structures[36–38]. For instance, an azobenzene compound composed of one hydrophobic core and four hydrophilic arms could self-assemble into micelles with controllable size and narrow dispersion in aqueous solution[39]. The DPM behavior of micelles showed high dependence on the micelle size. For larger micelles with diameter of *ca.* 520 nm (Fig. 6a), a significant deformation with the average axial ratio up to 4.5 was observed after irradiated for 5 min (Fig. 6c). In contrast, the average axial ratio of smaller colloids with diameter of 200 nm was still less than 2.0 under the same condition (Fig. 6b). Consequently, photo-induced deformation of the micelles showed positive size dependence in this case (Fig. 6d).

In our recent work, a series of narrow dispersed azopolymer microparticles with the size from 9 μm to 80 μm were prepared by combining the microfluidic technique with emulsion-solvent evaporation strategy[40]. On the contrary to above mentioned results, the microparticles with diameter of 9 μm showed the most significant deformation rate, while the microparticles with diameter of 80 μm showed the lowest deformation rate under the same irradiation condition (Figs. 6e–6h). The opposite tendencies should be attributed to the strong light absorbance of azobenzene. Both the calculation and measurement results confirmed that the light

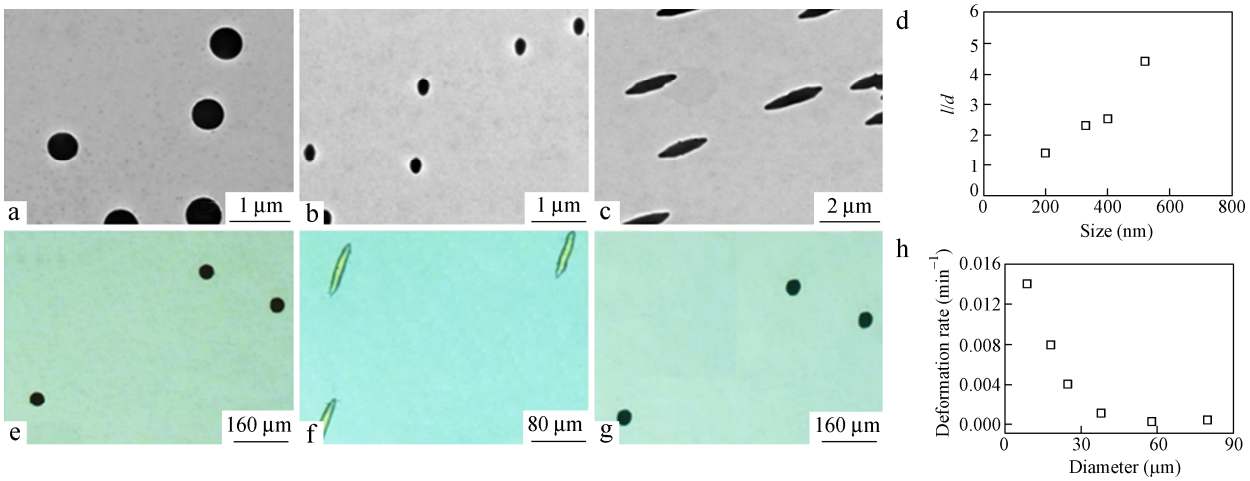


Fig. 6 TEM images of the colloidal spheres (a) before irradiation with average grain size of 520 nm and after being irradiated for 5 min with the initial average grain size of (b) 200 nm and (c) 520 nm, respectively; (d) relationship between the average axial ratio of the colloids and size (Reproduced with permission from Ref. [39]; Copyright (2015) American Chemical Society); (e) Optical microscopy image of the microparticles with average diameter of 58 μm; (f) optical microscopy image of the microparticles with initial diameter of 18 μm after irradiation for 7 h; (g) the microparticles with initial diameter of 58 μm after irradiation for 7 h; (h) relationship between the deformation rate and the initial particle sizes (Reproduced with permission from Ref. [40]; Copyright (2015) American Chemical Society)

https://doi.org/10.1007/s10118-018-2087-x

transmission intensity in azopolymer film became almost zero at the thickness around 800 nm[41]. The microstructures with dimension under 800 nm can be activated by LPL completely to achieve photo-induced mass migration, and therefore the driving force for DPM will be enhanced with the size of aggregates increasing. In contrast, photo-induced mass migration only occurs among the surface area of giant aggregates, and therefore larger size makes obstacle to the light-induced deformation. These results are in agree with our research results about the DPM of BFAs[32].

FUNCTIONALIZATION AND APPLICATIONS OF PHOTO-MANIPULATED PATTERNS

Determinate and sophisticated 3D azopolymer architectures are promising in both functionality and utilization. For instance, functional arrays with complex 3D architecture are available by templating from the deformed azopolymer patterns. These 3D patterns are expected to be applied as lithography masks, superhydrophobic surfaces, and photonic devices[42–44].

Etching Mask for Lithography

The facile and flexible DPM method affords predictable and deterministic manipulation on the shape and size of arrayed pores for various patterning applications, typically the etching masks for pattern transfer[33]. Following the process depicted in Fig. 7(a), the surface layer of pristine or deformed BFAs was peeled off and subsequently served as an etching mask (Figs. 7b–7d). Upon CF_4 etching for 10 min, definite porous structures were transferred onto the surface of silicon wafers. The obtained patterns were highly accordant to their corresponding polymeric masks (Figs. 7e–7g). These hexagonally arranged pores embedded on the silicon wafer showed great feasibility for preparing anisotropic surfaces and elaborate microreactor[45]. Furthermore, the photo-induced reshaping of pores can also be conducted after transferring the surface layer onto the silicon wafer, which provides readily photo-tunable masks to adapt the requirements of different etching applications.

Anisotropic Surface

The photo-induced deformation can also transform the pristine isotropic pattern into deformed structure with anisotropic properties. For instance, deformed patterns featured anisotropic wetting behavior on their surface[46]. As shown in Fig. 8, the initial water contact angle (CA) of fresh pattern corresponding to the image was 105° (Fig. 4b) and the surface was hydrophobic[34]. During the DPM by visible LPL irradiation, the CA value decreased with the irradiation time. After irradiated for 300 min, the cumulative decline was

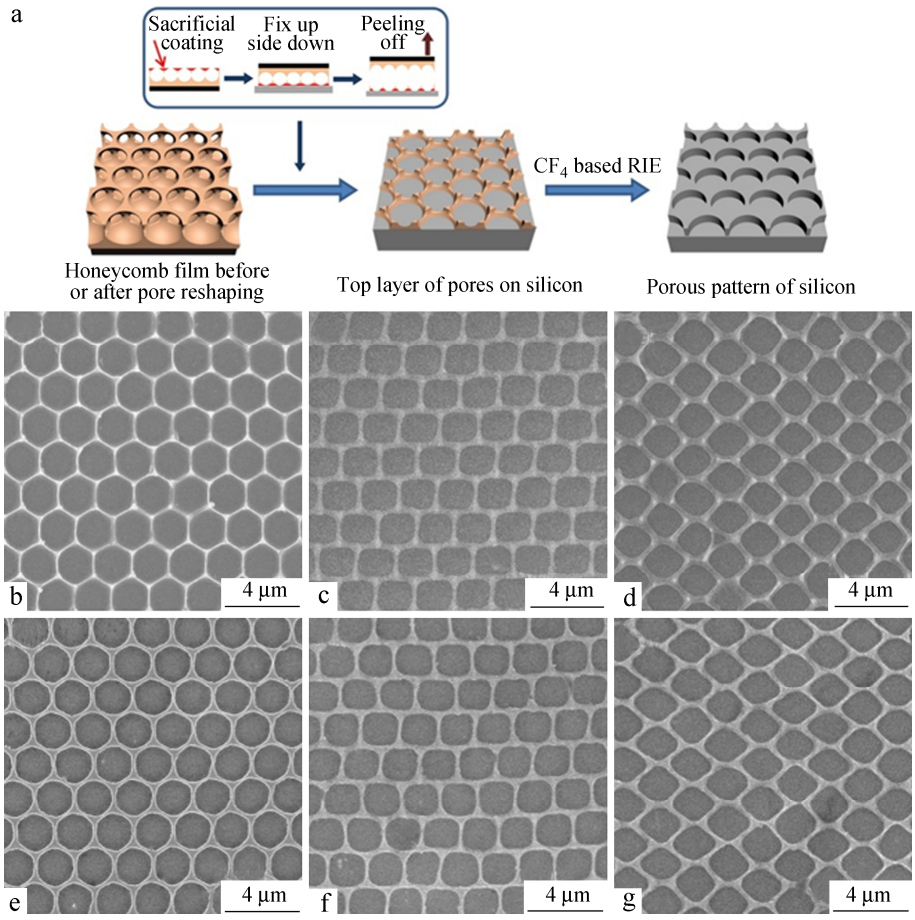


Fig. 7 (a) Scheme of the pattern transfer process from a honeycomb film to silicon wafer; (b–d) SEM images of inverted top layers on silicon with (b) round, (c) rectangular, and (d) rhombic pores; (e–g) SEM images of patterned silicon of (e) round, (f) rectangular, and (g) rhombic pores (Reproduced with permission from Ref. [33]; Copyright (2017) American Chemical Society)

https://doi.org/10.1007/s10118-018-2087-x

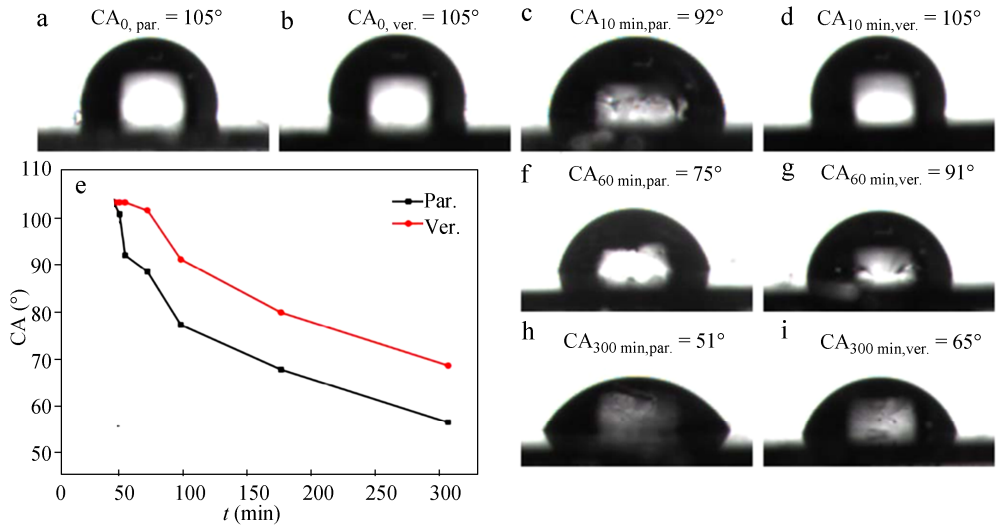


Fig. 8 Contact angle (CA) of azopolymer array (a, b) before and after LPL irradiation for (c, d) 10 min, (f, g) 60 min; and (h, i) 300 min parallel (par.) and vertical (ver.) to the polarized direction, respectively; (e) Relationship between CA and irradiation time parallel (par.) and vertical (ver.) to the polarized direction, respectively (Reproduced with permission from Ref. [34]; Copyright (2017) American Chemical Society)

around 54° and thus the surface turned to hydrophilic. The surface roughness of patterns was continually reduced by DMM. Thus, the transition from hydrophobic to hydrophilic achieved. In addition, the pattern showed roughness differential between polarization direction and orthogonal direction after DPM. The CA value decreased much slower along the orthogonal direction of polarization than that of parallel direction initially, and still kept about 14°–16° high after 60 min of irradiation. The anisotropic structure is promising in the field of photonic devices and oil-water separation[47, 48].

Shape Restoration

Interestingly, the transformed micropatterns after DPM can be apparently restored by subsequent irradiation after rotating the sample by 90° with an equal time intervals, demonstrating the versatility and restorability of DPM method. For example, starting from the rhombic pores (Fig. 3f) induced by LPL irradiation along *S* direction for 30 min, the BFAs with round pores (Fig. 9a) were almost recovered after subsequent irradiation along *V* direction for another 30 min[32]. The cross-section SEM image in Fig. 9(b) shows that the pores change from round to ellipse, indicating that the shrinkage along *Z* direction can tolerate the collapse during LPL irradiation induced transformation and restoration process. In another work of Descrovi *et al.*, blend of azopolymer (PAZO) and poly(methyl methacrylate) (PMMA) was employed to fabricate micropatterns with squared lattice of circular pillars through soft lithography technique[49]. A small fraction of passive component (PMMA) within a PAZO-PMMA mixture could significantly improve stiffness of the polymeric mixture under light illumination. Therefore, the improved mechanical property prevented the collapse of micropillars during DPM, and allowed reversible and controlled deformation by periodically tuning the laser polarization over several cycles. These tunable smart architectures presented here are promising in applications including photonic crystals, optical metamaterials, and dynamically wettable surfaces[50–52].

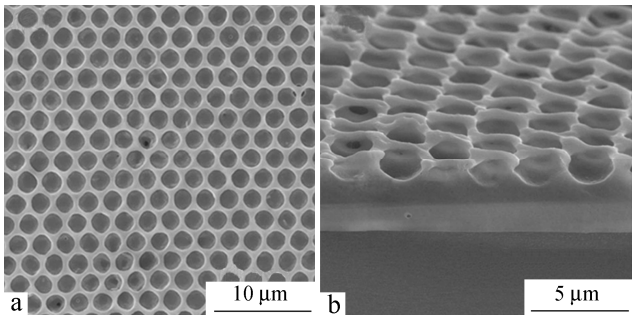


Fig. 9 SEM images of micropatterns after a secondary photo-manipulation: (a) top view; (b) cross-sectional view (Reproduced with permission from Ref. [32]; Copyright (2014) John Wiley and Sons, Inc.)

CONCLUSIONS AND OUTLOOK

As a light-controlled post modification technique, DPM is particularly suitable for the manipulation of self-assembled patterns in a noncontact and nondestructive manner. Combining the "bottom-up" self-assembly fabrication method with "top-down" DPM post modification approach, patterned structures with various features and functions can be readily fabricated. Thus, DPM technique is highly compatible with large-area, high-throughput fabrication processes and therefore provides a new route for surface patterning.

The fundamental of DPM relies on the property of photo-induced mass migration along the polarization direction. In molecular scale, this directionality is tightly relevant to the photo-induced alignment of azobenzene. However, the currently proposed theory cannot completely explain this unique directionality. The mechanism of DMM under glass transition temperature is still unclear. Therefore, the theoretical rationalization of DMM is essential for better understanding and operation of DPM. On the other hand, photo-fluidization effect in DPM causes the vertical collapse

https://doi.org/10.1007/s10118-018-2087-x

of microstructures that is unfavorable to the integrality of patterns. To avoid this effect, crosslinking can be employed to enhance the stability of polymeric network, but mass migration will also be restricted by crosslinking. New photo-responsive molecules are on demand to diminish the vertical collapse while maintaining the adequate reshaping speed. In addition, only homogenously reshaped patterns have been obtained by DPM processing until now. Light patterning with various intensity and distribution is reasonably interesting in the future. We believe that smart light irradiation and novel molecular design will significantly improve this area and bring much more opportunities for applications.

ACKNOWLEDGMENTS

This work was financially supported by the National Natural Science Foundation of China (Nos. 51622301 and 51573046), Projects of Shanghai Municipality (Nos. 14SG29 and 17JC400700) and Fundamental Research Funds for the Central Universities (No. 222201718002).

REFERENCES

1 Li, L.; Köpf, M. H.; Gurevich, S. V.; Friedrich, R.; Chi, L. Structure formation by dynamic self-assembly. Small 2012, 8(4), 488–503.
2 Nie, Z.; Kumacheva, E. Patterning furfaces with functional polymers. Nat. Mater. 2008, 7 (4), 277–290.
3 Huang, H.; Yi, G.; Zu, X.; Zhong, B.; Luo, H. Patterning of triblock copolymer film and its application for surface-enhanced raman scattering. Chinese J. Polym. Sci. 2017, 35(5), 623–630.
4 Biswas, A.; Bayer, I. S.; Biris, A. S.; Wang, T.; Dervishi, E.; Faupel, F. Advances in top-down and bottom-up surface nanofabrication: Techniques, applications & future prospects. Adv. Colloid Interface Sci. 2012, 170(1), 2–27.
5 Liu, X.; Yang, J.; Zha, L.; Jiang, Z. Self-assembly of hollow PNIPAM microgels to form discontinuously hollow fibers. Chinese J. Polym. Sci. 2014, 32(11), 1544–1549.
6 Ma, H.; Hao, J. Ordered patterns and structures *via* interfacial self-assembly: Superlattices, honeycomb structures and coffee rings. Chem. Soc. Rev. 2011, 40(11), 5457–5471.
7 Wang, D.; Möhwald, H. Template-directed colloidal self-assembly—the route to 'top-down' nanochemical engineering. J. Mater. Chem. 2004, 14(4), 459–468.
8 Li, J.; Shim, J.; Deng, J.; Overvelde, J. T.; Zhu, X.; Bertoldi, K.; Yang, S. Switching periodic membranes *via* pattern transformation and shape memory effect. Soft Matter 2012, 8(40), 10322–10328.
9 Yabu, H.; Jia, R.; Matsuo, Y.; Ijiro, K.; Yamamoto, S.; Nishino, F.; Takaki, T.; Kuwahara, M.; Shimomura, M. Preparation of highly oriented nano-pit arrays by thermal shrinking of honeycomb-patterned polymer films. Adv. Mater. 2008, 20(21), 4200–4204.
10 Zhou, J.; Sheiko, S. S. Reversible shape-shifting in polymeric materials. J. Polym. Sci., Part B: Polym. Phys. 2016, 54(14), 1365–1380.
11 Hu, Y.; Guo, W.; Kahn, J. S.; Aleman-Garcia, M. A.; Willner, I. A shape-memory DNA-based hydrogel exhibiting two internal memories. Angew. Chem. Int. Ed. 2016, 55(13), 4210–4214.
12 Wang, W.; Lin, J.; Cai, C.; Lin, S. Optical properties of amphiphilic copolymer-based self-assemblies. Eur. Polym. J. 2015, 65, 112–131.
13 Chen, D.; Liu, H.; Kobayashi, T.; Yu, H. Fabrication of regularly patterned microporous films by self-organization of an amphiphilic liquid-crystalline diblock copolymer in a dry environment. Macromol. Mater. Eng. 2010, 295(1), 26–31.
14 Li, Y.; He, Y.; Tong, X.; Wang, X. Photoinduced deformation of amphiphilic azo polymer colloidal spheres. J. Am. Chem. Soc. 2005, 127(8), 2402–2403.
15 Lee, S.; Kang, H. S.; Park, J. K. High-resolution patterning of various large-rea, highly ordered structural motifs by directional photofluidization lithography: Sub-30-nm Line, ellipsoid, rectangle, and circle arrays. Adv. Funct. Mater. 2011, 21(10), 1770–1778.
16 Lee, S.; Kang, H. S.; Park, J. K. Directional photofluidization lithography: Micro/nanostructural evolution by photofluidic motions of azobenzene materials. Adv. Mater. 2012, 24(16), 2069–2103.
17 Yu, H.; Kobayashi, T. Photoresponsive block copolymers containing azobenzenes and other chromophores. Molecules 2010, 15(1), 570–603.
18 Xing, Y.; Lin, S.; Lin, J.; He, X. Synthesis, self-assembly and responsive properties of PEG-*b*-PDMAEMA-*b*-PMMAzo triblock copolymers. Chinese J. Polym. Sci. 2013, 31(5), 833–840.
19 Hoersch, D. Let there be light: How to use photoswitchable cross-linker to reprogram proteins. Biochem. Soc. Trans. 2017, 45(3), 831–837.
20 Weis, P.; Wu, S. Light-switchable azobenzene-containing macromolecules: from UV to near infrared. Macromol. Rapid Commun. 2017, DOI: 10.1002/marc.201700220.
21 Goulet-Hanssens, A.; Utecht, M.; Mutruc, D.; Titov, E.; Schwarz, J.; Grubert, L.; Bléger, D.; Saalfrank, P.; Hecht, S. Electrocatalytic Z→E isomerization of azobenzenes. J. Am. Chem. Soc. 2017, 139(1), 335–341.
22 Zhao, Y.; Ikeda, T. Smart light-responsive materials: Azobenzene-containing polymers and liquid crystals. John Wiley & Sons: 2009.
23 Wang, H.; Lee, K. M.; White, T. J.; Oates, W. S. *Trans-cis* and *trans-cis-trans* microstructure evolution of azobenzene liquid-crystal polymer networks. Macromol. Theory Simul. 2012, 21(5), 285–301.
24 Bin, J.; Oates, W. S. A unified material description for light induced deformation in azobenzene polymers. Sci. Rep. 2015, 5, DOI: 10.1038/srep14654
25 Han, M.; Morino, S.; Ichimura, K. Factors affecting in-plane and out-of-plane photoorientation of azobenzene side chains attached to liquid crystalline polymers induced by irradiation with linearly polarized light. Macromolecules 2000, 33(17), 6360–6371.
26 Fang, G.; Maclennan, J.; Yi, Y.; Glaser, M.; Farrow, M.; Korblova, E.; Walba, D.; Furtak, T.; Clark, N. Athermal photofluidization of glasses. Nat. Commun. 2013, 4, DOI: 10.1038/ncomms2483
27 Yu, H. Photoresponsive liquid crystalline block copolymers: From photonics to nanotechnology. Prog. Polym. Sci. 2014, 39(4), 781–815.
28 Yu, H. Recent advances in photoresponsive liquid-crystalline polymers containing azobenzene chromophores. J. Mater. Chem. C 2014, 2(17), 3047–3054.
29 Karageorgiev, P.; Neher, D.; Schulz, B.; Stiller, B.; Pietsch, U.; Giersig, M.; Brehmer, L. From anisotropic photo-fluidity towards nanomanipulation in the optical near-field. Nat. Mater. 2005, 4(9), 699–703.
30 Gao, F.; Wang, W.; Li, X.; Li, L.; Lin, J.; Lin, S. Fabrication of ordered honeycomb amphiphobic films with extremely low fluorine content. J. Colloid Interface Sci. 2016, 468(15), 70–77

31 Zhang, A.; Bai, H.; Li, L. Breathfigure: A nature-inspired preparation method for ordered porous films. Chem. Rev. 2015, 115(18), 9801–9868.
32 Wang, W.; Du, C.; Wang, X.; He, X.; Lin, J.; Li, L.; Lin, S. Directional photomanipulation of breath figure arrays. Angew. Chem. Int. Ed. 2014, 53(45), 12116–12119.
33 Wang, W.; Yao, Y.; Luo, T.; Chen, L.; Lin, J.; Li, L.; Lin, S. Deterministic reshaping of breath figure arrays by directional photomanipulation. ACS Appl. Mater. Interfaces 2017, 9(4), 4223–4230.
34 Kong, X.; Wang, X.; Luo, T.; Yao, Y.; Li, L.; Lin, S. Photomanipulated architecture and patterning of azopolymer array. ACS Appl. Mater. Interfaces 2017, 9(22), 19345–19353.
35 Lee, S.; Shin, J.; Lee, Y. H.; Park, J. K. Fabrication of the funnel-shaped three-dimensional plasmonic tip arrays by directional photofluidization lithography. ACS nano 2010, 4(12), 7175–7184.
36 Li, C.; Wang, W.; Wang, X.; Jiang, H.; Zhu, J.; Lin, S. Fabrication of porous polymer microspheres by tuning amphiphilicity of the polymer and emulsion-solvent evaporation processing. Eur. Polym. J. 2015, 68, 409–418.
37 Wang, Y.; Lin, S.; Zang, M.; Xing, Y.; He, X.; Lin, J.; Chen, T. Self-assembly and photo-responsive behavior of novel ABC 2-type block copolymers containing azobenzene moieties. Soft Matter 2012, 8(11), 3131–3138.
38 Lin, S.; Wang, Y.; Cai, C.; Xing, Y.; Lin, J.; Chen, T.; He, X. Tuning self-assembly and photo-responsive behavior of azobenzene-containing triblock copolymers by combining homopolymers. Nanotechnology 2013, 24(8), DOI: 10.1088/0957-4484/24/8/085602
39 Wang, J.; Wang, S.; Zhou, Y.; Wang, X.; He, Y. Fast photoinduced large deformation of colloidal spheres from a novel 4-arm azobenzene compound. ACS Appl. Mater. Interfaces 2015, 7(30), 16889–16895.
40 Li, J.; Chen, L.; Xu, J.; Wang, K.; Wang, X.; He, X.; Dong, H.; Lin, S.; Zhu, J. Photoguided shape deformation of azobenzene-containing polymer microparticles. Langmuir 2015, 31(48), 13094–13100.
41 Kang, H. S.; Lee, S.; Lee, S. A.; Park, J. K. Multilevel micro/nano texturing by three dimensionally controlled photofluidization and its use in plasmonic applications. Adv. Mater. 2013, 25(38), 5490–5497.
42 Choi, J.; Cho, W.; Jung, Y. S.; Kang, H. S.; Kim, H. T. Direct fabrication of micro/nano-patterned surfaces by vertical-directional photofluidization of azobenzene materials. ACS Nano 2017, 11(2), 1320–1327.
43 Sun, P. Z.; Liu, Z.; Wang, W.; Ma, L. L.; Shen, D.; Hu, W.; Lu, Y.; Chen, L.; Zheng, Z. G. Light-reconfigured waveband-selective diffraction device enabled by micro-patterning of a photoresponsive self-organized helical superstructure. J. Mater. Chem. C 2016, 4(39), 9325–9330.
44 Gao, Y.; Li, A.; Gu, Z.; Wang, Q.; Zhang, Y.; Wu, D.; Chen, Y.; Ming, N.; Ouyang, S.; Yu, T. Fabrication and optical properties of two-dimensional ZnO hollow half-shell arrays. Appl. Phys. Lett. 2007, 91(3), DOI: 10.1063/1.2759268
45 Wiktor, P.; Brunner, A.; Kahn, P.; Qiu, J.; Magee, M.; Bian, X.; Karthikeyan, K.; LaBaer, J. Microreactor array device. Sci. Rep. 2015, 5, 8736.
46 Oscurato, S. L.; Borbone, F.; Maddalena, P.; Ambrosio, A. Light-driven wettability tailoring of azopolymer surfaces with reconfigured three-dimensional posts. ACS Appl. Mater. Interfaces 2017, 9(35), 30133–30142.
47 Phillips, K. R.; Vogel, N.; Hu, Y.; Kolle, M.; Perry, C. C.; Aizenberg, J. Tunable anisotropy in inverse opals and emerging optical properties. Chem. Mater. 2014, 26(4), 1622–1628.
48 Gu, J.; Xiao, P.; Chen, J.; Zhang, J.; Huang, Y.; Chen, T. Janus polymer/carbon nanotube hybrid membranes for oil/water separation. ACS Appl. Mater. Interfaces 2014, 6(18), 16204–16209.
49 Pirani, F.; Angelini, A.; Frascella, F.; Rizzo, R.; Ricciardi, S.; Descrovi, E. Light-driven reversible shaping of individual azopolymeric micro-pillars. Sci. Rep. 2016, 6, DOI: 10.1038/srep31702
50 Hong, J. C.; Park, J. H.; Chun, C.; Kim, D. Y. Photoinduced tuning of optical stop bands in azopolymer based inverse opal photonic crystals. Adv. Funct. Mater. 2007, 17(14), 2462–2469.
51 Arbabi, A.; Horie, Y.; Bagheri, M.; Faraon, A. Dielectric metasurfaces for complete control of phase and polarization with subwavelength spatial resolution and high transmission. Nat. Nanotechnol. 2015, 10(11), 937–943.
52 Zillohu, A. U.; Abdelaziz, R.; Homaeigohar, S.; Krasnov, I.; Müller, M.; Strunskus, T.; Elbahri, M. Biomimetic transferable surface for a real time control over wettability and photoerasable writing with water drop lens. Sci. Rep. 2014, 4, DOI: 10.1038/srep07407